Internal Momentum State Mapping Using High Harmonic Radiation

Xinhua Xie,[1] Armin Scrinzi,[1] Marlene Wickenhauser,[1] Andrius Baltuška,[1] Ingo Barth,[2] and Markus Kitzler[1,*]

[1]*Photonics Institute, Vienna University of Technology, Vienna, Austria, EU*

[2]*Institute for Physical and Theoretical Chemistry, Free University of Berlin, Berlin, Germany, EU*

(Received 1 February 2008; published 17 July 2008)

We numerically demonstrate so-far undescribed features in ionization and high harmonic generation from bound states with nonvanishing electronic angular momentum. The states' modified response to a strong laser pulse can be exploited for novel measurement and pulse production schemes. It is shown that angularly asymmetric tunneling from the states can be mapped onto variations of high harmonic intensities and that near-circularly polarized isolated attosecond extreme ultraviolet or x-ray pulses can be produced.

DOI: 10.1103/PhysRevLett.101.033901 PACS numbers: 42.65.Ky, 32.80.Rm, 42.65.Re

The way gas molecules respond to a strong laser field depends on their internal state. This fact has been exploited in a range of recent experiments, where insight into the bound electron structure, nuclear dynamics, and even electronic dynamics was gained from measurements of photon or electron spectra [1]. The emission of photons via high-order harmonic generation (HHG) from aligned molecules has especially attracted a lot of attention recently, e.g., [2–9]. It is even possible to infer information about the internal attosecond bound dynamics from the high harmonic (HH) spectrum [10,11].

In this Letter we demonstrate a conceptually reversed approach: instead of extracting information about the bound state from the HH radiation, we prepare the molecular state in order to control the properties of the HH emission. Specifically we consider electronic ring currents, which can be excited in a suitable molecule or atom by (weak) circularly polarized π pulses [12,13]. We show that the HH radiation created from such systems by irradiation with a second strong pulse exhibits unique features that can be exploited for measurements and pulse generation: (i) ionization and laser-controlled rescattering can be used to probe the systems' internal symmetry and (ii) spatially and temporally coherent, nearly circularly polarized, extreme ultraviolet (XUV) or x-ray single attosecond pulses can be produced.

The initial ring-current states $|E_\pm\rangle = 1/\sqrt{2}(|E_1\rangle \pm i|E_2\rangle)$ that we use are eigenstates of angular momentum L_z with respect to the axis perpendicular to the (x, y) plane with eigenvalues $\pm|m|$. The states are constructed in an axially symmetric system by superposition of two equally populated, degenerate real states of m-fold angular symmetry ($|m| \geq 1$), denoted by $|E_1\rangle$ and $|E_2\rangle$, respectively, with wave functions $\Psi_1(\rho, \varphi) = f(\rho) \times \cos(|m|\varphi)$ and $\Psi_2(\rho, \varphi) = f(\rho)\sin(|m|\varphi)$, from which one obtains the ring-current wave functions $\Psi_\pm(\rho, \varphi) = 1/\sqrt{2} f(\rho) e^{\pm i|m|\varphi}$. Here we use 2D polar coordinates $(x, y) = (\rho\cos\varphi, \rho\sin\varphi)$ and atomic units. Because only the phase of the wave function depends on φ, the electron density $|\Psi_\pm|^2$ of a ring-current state $|E_\pm\rangle$ is constant as a function of φ. It is independent of the current's left-handed $(+)$ or right-handed $(-)$ direction, which can be induced by an anticlockwise or clockwise rotating circular optical π pulse, respectively [12,13].

To study ionization dynamics of and high harmonic generation from ring-current states we numerically solve the time-dependent Schrödinger equation in two spatial dimensions for a single active electron coupled to the laser electric field in dipole approximation. For our simulations we use a rotationally symmetric, short-range smoothed ring-shaped molecular potential with a radius $R = 3$, whose radial dependence is given by $V(\rho) = -[1 + \exp(-(\rho/2R)^8)]/\sqrt{(\rho - R)^2 + a^2}$. The shielding parameter is chosen as $a = 0.65$, yielding a binding energy of 9.5 eV for the state $|m| = 6$, which we will exclusively use to demonstrate our results, although in our simulations we also used different ring-current states with angular momenta $|m| = \{1, \ldots, 6\}$.

We first investigate electron detachment from a molecule in a ring-current state. Figure 1 shows snapshots of the electron density in a laser pulse, linearly polarized in x, at a wavelength of 1600 nm and pulse duration of 10 fs FWHM (Gaussian intensity envelope). The insets of Figs. 1(a) and 1(b) show the electron density for initial states $|E_1\rangle$ and $|E_2\rangle$, respectively. The nodes in the electron density are imprinted also in the detached part of the wave function: There are either 3 or 2 lobes of electron density, depending on the angular nodal distribution perpendicular to the ionizing direction, as expected for molecular tunnel ionization [14]. When the two states are superimposed to form the state $|E_+\rangle$, the probability density inside the molecule becomes radially constant; any nodal structure is absent, cf. inset of Fig. 1(c). Ionization of this ring-current state by the same linearly polarized field as in 1(a) and 1(b) results in the emittance of an electronic wave packet strongly rotated off the polarization axis in the counterclockwise direction, i.e., along the direction of the ring current; see Fig. 1(c). Correspondingly, ionization from a state $|E_-\rangle$

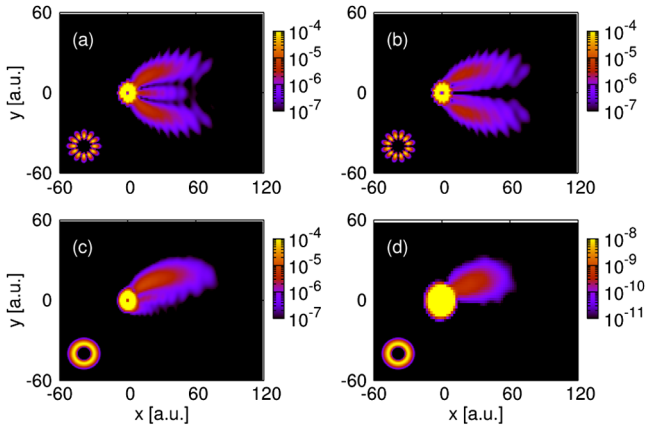

FIG. 1 (color online). Snapshots of the probability density of an electron wave packet as it is detached from a ring-current state by strong-field ionization in a linearly polarized laser field. Ionization from state (a) $|E_1\rangle$, (b) $|E_2\rangle$, (c) $|E_+\rangle = 1/\sqrt{2}(|E_1\rangle + i|E_2\rangle)$. (d) Same as (c) but for a weaker field.

results in wave packet emission into the opposite, clockwise, direction (not shown).

Because creation of XUV radiation necessitates strong fields we used a peak field intensity of 5.6×10^{13} W/cm^2, which places Figs. 1(a)–1(c) into the regime of barrier suppression ionization. However, the effect of asymmetric emission is also observed at the much lower peak intensity of 1×10^{13} W/cm^2, where ionization occurs only by tunneling; see Fig. 1(d).

At first glance this *asymmetric* emission from a rotationally *symmetric* electron density distribution could be surprising, since structures in electron emission reported so far have their counterparts in structures in the molecule's bound electron density [14–19]. A simple classical picture for the asymmetry observed here is that during ionization internal angular momentum is imparted to the detached electron. This statement is corroborated by our simulations, which show a monotonic increase of the detached electron's transverse momentum with increasing $|m|$.

In more accurate quantum mechanical terms, the effect of asymmetric emission is due to the interference of two wave functions emitted from the two initial state components, which have opposite parity with respect to reflections about the x axis. The electron density in Fig. 1(a) has a maximum along $x = 0$, while Fig. 1(b) shows a node. The coherent superposition of these two wave packets produces the pattern in emission shown in Figs. 1(c) and 1(d), where the density at $y < 0$ is suppressed by destructive interference.

Next we investigate HH spectra generated from ring-current states. As ionization is the first step in the three-step process [1] of HH generation, observed harmonic spectra should be sensitive to the ring-current state and thus to the direction of the ring current as given by the sign of the quantum phase $\pm|m|\varphi$. For symmetry reasons, however, harmonic intensity spectra from ring-current states in a linearly polarized laser pulse are insensitive to sgn(m). By using elliptically polarized laser fields $\vec{\mathcal{E}}(t) = \mathcal{E}_0(t) \times [\cos(\omega t)\vec{e}_x + \varepsilon \sin(\omega t)\vec{e}_y]$, with $\mathcal{E}_0(t)$ the pulse envelope, ω the laser frequency, and ε the ellipticity, respectively, we can break that symmetry and probe the transversal momentum distribution of the tunneling wave packets using HH spectra. Figure 2(a) shows high harmonic spectra from the same ring-current state and with the same pulse parameters as used for Fig. 1, except that the ellipticity of the pulse is varied. One sees some variation of the cutoff frequency and significant variations of intensity. The variations in the cutoff frequency are consistent with the variations of the classical recollision energies in the simple man's model of HHG [1]. The intensity variations reflect the transverse distribution of electron momentum at emission as follows: The field component $\mathcal{E}_\perp$ perpendicular to the main polarization axis can compensate an initial transverse momentum $p_\perp(t')$ of the electrons and guide them back to the nucleus. By varying the ellipticity we steer the recollision current across the target, thereby imaging the distribution of transverse tunneling electron momenta. A similar idea was proposed recently to control high harmonic generation in atoms [20]. There it is shown that for small ellipticities ε the transverse displacement by the $\mathcal{E}_\perp$ depends linearly on ε. By treating the electrons as classical particles, one can calculate the ellipticity needed to compensate an initial momentum $p_\perp(t')$ as $\varepsilon \approx \alpha p_\perp(t')$. For our pulse parameters we obtain $\alpha \approx 0.5$. Figure 2(b) compares harmonic intensity at the cutoff as a function of ε (dotted line, upper abscissa) to the initial transverse mo-

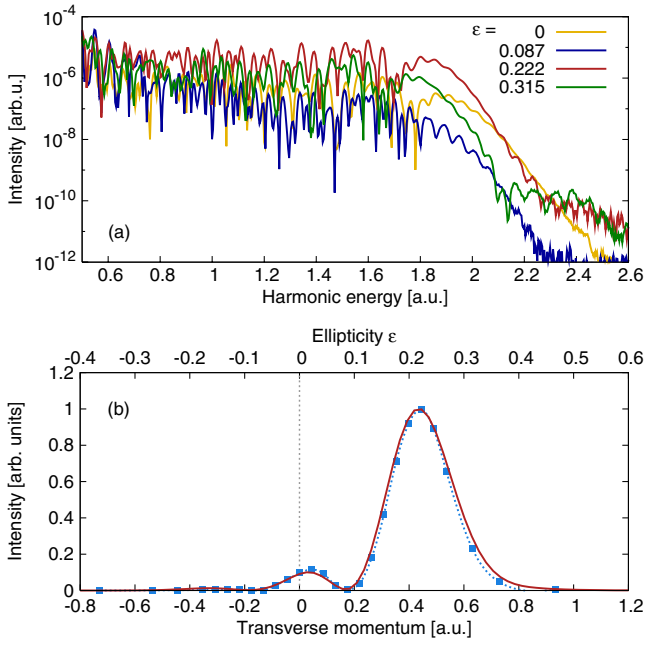

FIG. 2 (color online). (a) HH spectra from a ring-current state $m = +6$ for different ellipticities ε, (b) comparison of the HH intensity in the cutoff as a function of ellipticity ε (dots) with the distribution of transverse electron momenta $p_\perp$ at the birth time for the highest harmonics (full line). Both curves were normalized to peak values of 1.

mentum (full line, lower abscissa). The transverse momentum distribution at release time $p_\perp(t')$ was determined from the numerically exact wave function using the probing technique of Ref. [21]. The distribution of harmonic intensity found by varying the ellipticity matches almost exactly the initial momentum distribution with the linear coefficient of $\alpha \approx 0.5$. The momentum distribution is asymmetric with respect to the origin and peaks at a positive value as expected from the previously described ionization mechanism for a ring-current state with $\mathrm{sgn}(m) = +1$, thus demonstrating the sensitivity of the proposed measurement scheme to the sign of the quantum phase. The method can be used in general to perform all-optical measurements of momentum distributions of tunneling wave packets without the need for more complicated methods based on position- and time-sensitive electron detection. As the present method offers subcycle temporal resolution, it can also be applied to probe the effects of fast internal electron dynamics on ionization.

Now we turn to a novel application of $|m| \geq 1$ states for the generation of high harmonic pulses. Radiation created by HHG from atoms is—due to symmetry considerations—polarized in the same direction as the driving laser polarization. In aligned molecules the polarization direction of the emitted radiation differs, in general, from that of the driving light [9]. However, elliptically (circularly) polarized harmonics cannot be produced by simply using elliptical (circular) driving polarization, because this leads to the suppression of recollision and a dramatic drop in photon yield [1]. In a range of schemes this problem is dealt with by meticulously shaping the polarization of the drive pulse; see, e.g., Ref. [22] and references therein. Here we demonstrate the reversed approach and use linear drive laser polarization, but prepare the molecules in ring-current states instead, which leads to the appearance of nearly circular polarized high harmonics. The resultant effect could be understood as a specific form of circular dichroism on the single-molecule level (for a discussion of circular dichroism in the strong-field context see, e.g., [23]).

In Fig. 3(a) we show the high harmonic intensity spectrum of the two orthogonal polarization components, $I_x(\omega)$ and $I_y(\omega)$, for the case of linear drive polarization, $\varepsilon = 0$, whose total intensity $I = I_x + I_y$ is given by the light gray (yellow) line in Fig. 2(a). The intensity I_x for harmonic polarization parallel to the field direction at laser peak and I_y perpendicular to it are comparable, especially in the cutoff around 1.9 a.u. with a ratio in intensity of 1:4. The two components are out of phase by about $\pi/2$ over a broad spectral range (gray dots in Fig. 3). This means that those harmonics correspond to near-circularly polarized XUV radiation, with a ratio of ~1:2 between the smallest and the largest field components. The intensity of the pulse can be enhanced by nearly an order of magnitude by the use of a slightly elliptically polarized driver with $\varepsilon \approx 0.2$ [see Fig. 2(b)].

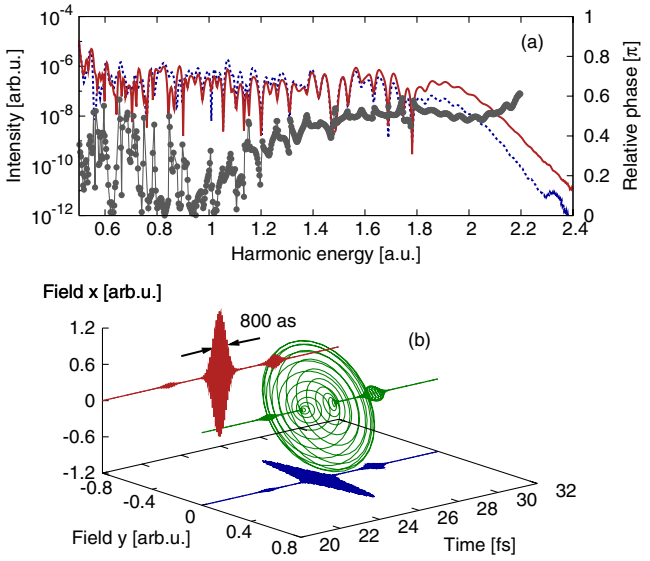

FIG. 3 (color online). (a) HH spectra of I_x (full red line) and I_y (dashed blue line) and their relative phase (gray dots) from a ring-current state with $m = +6$. Pulse parameters as in Fig. 2 for linear laser polarization. (b) Nearly circularly polarized electric field of an attosecond pulse obtained by filtering the highest harmonics of the spectra shown in (a).

The availability of (near-)circularly polarized subfemtosecond pulses at short wavelengths via high harmonic generation may open the door to tabletop-scale imaging and spectroscopy of ferromagnetic materials using magnetic x-ray absorption spectroscopy, e.g., [24], x-ray circular magnetic dichroism, e.g., [25], and x-ray resonance magnetic scattering, e.g., [26], and at the same time push the temporal resolution of those methods to extreme time scales.

A simple calculation in the frame of the strong-field approximation elucidates the mechanism of production of circularly polarized HH radiation. Within the strong-field approximation, the high frequency dipole response at time t is obtained as a product of the three probability amplitudes for ionization, propagation, and recombination [27]. The polarization state of the harmonic radiation is determined by the recombination step. At frequency $\omega(\vec{k}(t)) = \vec{k}^2(t)/2 + I_p$ it is proportional to the bound-free dipole matrix element $\langle \Psi_m | \vec{r} | \vec{k}(t) \rangle$, where the incident electron wave vector $\vec{k}$ of the plane waves $|\vec{k}(t)\rangle$ points in the direction of the drive field. Writing the ring-current wave function in cylindrical coordinates $\Psi_m = f(\rho) e^{im\varphi}$, assuming linearly polarized laser light in x, such that the vector of recollision $\vec{k} = k\vec{e}_x$ and applying the Bessel expansion $e^{ik\rho\cos\varphi} = \sum_n i^n e^{in\varphi} J_n(k\rho)$ one easily sees that the x and y components of the harmonic radiation at frequency $\omega(k)$ are $(\epsilon_x, \epsilon_y) \propto (B_{m+1} - B_{m-1}, iB_{m+1} + iB_{m-1})$, where we have defined the integral $B_m := \langle f(\rho) | \rho | J_m(k\rho) \rangle$. This integral varies rapidly as a function of m, if the rescattering wavelength is comparable to the extension of the initial bound state $\Delta\rho$ such that $2\pi/k \sim \Delta\rho$. For the case of a

wave function with Gaussian radial shape, the extension is defined as $f(\rho) = \exp(-(\rho - R/2)^2/\Delta\rho^2)$. Then the two polarization components are dominated by one of the integrals, either B_{m+1} or B_{m-1}. Together with the relative phase of $\pi/2$ due to the factor i, which is present for both possibilities, one obtains strongly elliptical, nearly circular polarization.

This simple analysis shows that creation of circularly (elliptically) polarized harmonics is a generic effect, which appears for any system with $|m| \geq 1$ and harmonic frequencies in the range $\omega \sim 2\pi^2/\Delta\rho^2 + I_p$. As neutral molecular ring-current systems have binding energies below 10 eV, one uses drive pulses with lower laser peak intensities but longer wavelengths to avoid excessive ionization. To reach harmonic photon energies beyond the XUV range, i.e., x rays, it is, however, unavoidable to apply high peak intensities, and ionic systems will have to be used.

In an intuitive picture, production of circularly polarized attosecond pulses via HHG proceeds as follows: First, angular momentum is transferred to the system which can be achieved by any method, for example, by a (weak) circularly polarized optical pump pulse [12,13]. Then the angular momentum is ''readout'' by the returning electron wave packet in strong-field recollision. For long-lived angular states, the first step is decoupled from the second one, which can happen at any time later. This is reminiscent of the laser principle, where first population inversion is created by any suitable method, which later on can be recovered in a controlled way, e.g., in a short burst.

For experimental applications one must worry about the achievable harmonic intensities. For that we made a comparison with the standard HHG with linearly polarized laser pulses and an $m = 0$ state of a model atom with the same ionization potential, for which we find the same yield of cutoff harmonics within a factor of ~ 2.

Finally, we may note that although for technical reasons we have used the $|m| = 6$ state of our model potential throughout, all our findings are of general nature and equally valid even for $|m| = 1$. Furthermore, thus far we have kept our discussions general and independent of any specific molecular or atomic system. Possible candidates for an experimental implementation of our schemes are derivatives of benzene, for which the lowest degenerate states $|E_{1,2}\rangle$ have a binding energy of about 6 eV and can be excited from the ground state by the second harmonic of Ti:sapphire.

In conclusion, we have demonstrated that ring-current initial states lead to nonstandard ionization and HHG by strong laser pulses. First, it was shown that the internal state is transferred to the tunneling wave packets, which receive an initial momentum kick, a so-far unexplored mechanism. The direction of the kick is determined by the sign of the bound state's phase. Second, to measure this effect we introduced a general method for mapping the transversal momentum distribution of tunneling wave packets by all-optical technology, which uncovers the pronounced asymmetry in the momentum spectrum. Third, it was demonstrated that during the recombination process the internal state is transferred to the polarization state of the emitted photons, which leads to the production of novel, spatially and temporally coherent, nearly circularly polarized attosecond XUV or x-ray pulses. These pulses might open the door to tabletop-scale imaging and spectroscopy of ferromagnetic materials on extreme time scales.

Fruitful discussions with S. Gräfe and O. D. Mücke are gratefully acknowledged. This work was partly financed by the Austrian Science Fund, Grants SFB016 and U33-16, and Deutsche Forschungsgemeinschaft, project Ma 515/23-1.

*Corresponding author.
markus.kitzler@tuwien.ac.at

[1] P. B. Corkum and F. Krausz, Nature Phys. **3**, 381 (2007).
[2] T. Kanai, S. Minemoto, and H. Sakai, Nature (London) **435**, 470 (2005).
[3] C. Vozzi *et al.*, Phys. Rev. Lett. **95**, 153902 (2005).
[4] R. Torres *et al.*, Phys. Rev. Lett. **98**, 203007 (2007).
[5] J. Itatani *et al.*, Phys. Rev. Lett. **94**, 123902 (2005).
[6] R. Velotta *et al.*, Phys. Rev. Lett. **87**, 183901 (2001).
[7] J. Itatani *et al.*, Nature (London) **432**, 867 (2004).
[8] T. Kanai, S. Minemoto, and H. Sakai, Phys. Rev. Lett. **98**, 053002 (2007).
[9] J. Levesque *et al.*, Phys. Rev. Lett. **99**, 243001 (2007).
[10] H. Niikura, D. M. Villeneuve, and P. B. Corkum, Phys. Rev. Lett. **94**, 083003 (2005).
[11] M. Kitzler *et al.*, Phys. Rev. A **76**, 011801(R) (2007).
[12] I. Barth *et al.*, J. Am. Chem. Soc. **128**, 7043 (2006).
[13] I. Barth and J. Manz, Phys. Rev. A **75**, 012510 (2007).
[14] X. M. Tong, Z. X. Zhao, and C. D. Lin, Phys. Rev. A **66**, 033402 (2002).
[15] I. V. Litvinyuk *et al.*, Phys. Rev. Lett. **90**, 233003 (2003).
[16] D. Pavičić *et al.*, Phys. Rev. Lett. **98**, 243001 (2007).
[17] A. S. Alnaser, Phys. Rev. Lett. **93**, 113003 (2004).
[18] J. Muth-Böhm, A. Becker, and F. H. M. Faisal, Phys. Rev. Lett. **85**, 2280 (2000).
[19] G. L. Kamta and A. D. Bandrauk, Phys. Rev. A **74**, 033415 (2006).
[20] N. Dudovich *et al.*, Phys. Rev. Lett. **97**, 253903 (2006).
[21] X. Xie *et al.*, Phys. Rev. A **76**, 023426 (2007).
[22] D. B. Milošević, W. Becker, and R. Kopold, Phys. Rev. A **61**, 063403 (2000).
[23] N. Manakov *et al.*, J. Phys. B **36**, R49 (2003).
[24] S. W. Lovesey and S. P. Collins, *X-Ray Scattering and Absorption by Magnetic Materials* (Oxford University, New York, 1996).
[25] F. Nolting *et al.*, Nature (London) **405**, 767 (2000).
[26] J. Chakhalian *et al.*, Nature Phys. **2**, 244 (2006).
[27] M. Y. Ivanov, T. Brabec, and N. Burnett, Phys. Rev. A **54**, 742 (1996).